PAPER

Cirsium Japonicum DC ingredients-loaded silk fibroin nanofibrous matrices with excellent hemostatic activity

Biomedical Physics & Engineering Express

PAPER

Cirsium Japonicum DC ingredients-loaded silk fibroin nanofibrous matrices with excellent hemostatic activity

RECEIVED
9 November 2017

REVISED
23 January 2018

ACCEPTED FOR PUBLICATION
31 January 2018

PUBLISHED
16 February 2018

Linlin Ma[1,2], **Dongdong Zhang**[1,2], **Xingxing Yang**[1,2], **Lin Zhang**[3], **Jin Chu**[1,2], **Guoyin Kai**[4,5], **Chuanglong He**[2], **Xiumei Mo**[2] and **Hongsheng Wang**[1,2,5]

[1] Key Laboratory of Science & Technology of Eco-Textile, Ministry of Education, Donghua University, Shanghai 201620, People's Republic of China
[2] Biomaterials and Tissue Engineering Lab, College of Chemistry, Chemical Engineering and Biotechnology, Donghua University, Shanghai 201620, People's Republic of China
[3] Department of Pharmacy, Shaoxing People's Hospital, Shaoxing Hospital of Zhejiang University, Shaoxing, Zhejiang, 31200, People's Republic of China
[4] Institute of Plant Biotechnology, Development Center of Plant Germplasm Resources, College of Life and Environment Sciences, Shanghai Normal University, Shanghai 200234, People's Republic of China
[5] Authors to whom any correspondence should be addressed.

E-mail: gykai@shnu.edu.cn **and** whs@dhu.edu.cn

Keywords: silk fibroin, Cirsium Japonicum DC, green electrospinning, hemostatic dressing

Abstract

Regenerated Silk fibroin (SF) from *Bombyxmori* has emerged in recent years as candidates for wound dressing due to its excellent biocompatibility and low inflammatory response. Cirsium Japonicum DC (CJDC) is a kind of Chinese herb medicine with evident hemostatic and anti-inflammatory analgesic effect. In this study, we aimed to manufacture a novel green electrospun SF nanofibrous matrice loading ingredients extracted from CJDC which should be useful in hemostasis as well as wound healing. FTIR spectra showed that the CJDC extracts were successfully loaded into the SF nanofibrous matrices, which appeared morphology of porous mesh structure. The as-prepared matrices inherited the good skin affinity and hemocompatibility of SF, as indicated by the skin cell viability assay and hemolysis test *in vitro*. Furthermore, according to the results of plasma recalcification profiles test, the incorporation of CJDC extracts significantly improved the hemostatic performance of SF nanofibrous matrices. Interestingly, the SF nanofibrous matrices loading CJDC components extracted by petroleum ether (peE-CJDC@SF) showed the best antihemorrhagic activity among the tested samples (with astringent time of 9.5 min), even better than some clinically used products such as absorbable gelatin sponge (AGS) and aseptic hemostyptic gauze (AHG). Our findings suggested the peE-CJDC@SF nanofibrous matrices could be a promising candidate using as hemostatic material and wound dressing.

1. Introduction

Traditional medical dressings which origin from cotton crop has chronically been widely used in various types of trauma care due to its good moisture retention, alkali resistance and thermostability [1, 2]. However, the traditional dressings have little hemostatic effect, and is incapable of keeping the wound wetting, which prevented the growth of epithelial cells, and thus delayed wound healing. In addition, it usually causes second damage to wound when changing dressings, which is due to the regenerative epithelial cells growing into the dressings [3]. Thus, it is a better choice to develop biodegradable dressings with good moisturizing and hemostatic performances for wound healing.

As hemorrhage is an inevitable complication after trauma in daily life, the application of topical hemostatic materials is important [4]. Various hemostatic materials have been developed in recent years [5]. For example, the medical dressing made of chitosan has good hemostatic effect and antibacterial property, which has made it a common hemostyptic material [6–8]. But its promotion is a big problem because of its poor solubility in most general solvents and causing allergic reactions for people allergy to seafood [9–11]. Fibrin sealant (FS) is another commonly used hemostatic materials which is able to promote wound

healing and applied to patients with blood coagulation disorder [12, 13]. However, the use of FS requires auxiliary equipment, which increase the difficulty of transport and storage, and is not suitable for the rescue in battle field and other emergency scenes[13–16].

Regenerated silk fibroin (SF) was a natural polymer which can be obtained conveniently [17, 18]. SF has low immunogenicity, good biocompatibility and moisturizing performance [19–22]. Dressings based on SF attracted much attention in recent years [23]. Although hemostasis can be achieved by using varies form of SF dressing [24, 25], their hemostatic performance still need to improve to meet the higher requirement. Cirsium Japonicum DC (CJDC) is a plant which belongs to Compositae. Because of its variety of medical effects (including hemostasis, anti-inflammatory, and antitumor), CJDC has been one of the commonly used herbs in traditional Chinese medicines [26–29]. The main medicinal components of CJDC included total flavonoid, essential oil, lipid, saccharides, etc [26–29]. Among them, flavonoid has been proven to be the main ingredients responsible for the hemostatic activity in CJDC [26–29]. It is reasonable the combination of CJDC and SF could provide a better option for wound dressings. According to our previous studies, the green electrospun SF nanofibrous matrices have high specific surface areas and porosity as well as good skin affinity [30]. Here, we attempted to develop a novel green electrospun SF nanofibrous matrice loading pharmacological constituents of CJDC for wound healing. As the pharmacological efficacy of CJDC vary depending on the different solvent used for the extraction [31], the ingredients extracted with different methods were used to prepare the SF composite nanofibers respectively in the present study. Subsequently, the SF nanofibrous matrices loading different extracts of CJDC were characterized in physical and chemical properties and evaluated on the biocompatibility and hemostatic performance by scanning electronic microscopy (SEM), cell viability and plasma recalcification profiles assays.

2. Experimental sections

2.1. Material

Cocoon of *Bombyxmorisilkworm* was purchased from Jiaxing Silk Co. (China). CJDC was purchased from Kangyuan Chinese medicine health square CO. (China). Polyethylene oxide (PEO, Mw = 900 000) was purchased from Sigma–Aldrich China Inc. The absorbable gelatin sponge (AGS) was purchased from JinLing Pharmary CO. (China). The aseptic hemostatic gauze (AHG) was purchased from Hainuo Co. (China). L929 cells were provided by Institute of Biochemistry and Cell Biology (Chinese Academy of Sciences, China). Other chemicals were all of analytical grade or higher and used as received. Ultrapure water used throughout the whole research.

2.2. Extraction of the hemostatic components from the CJDC

CJDC (30 g) was ground into powder and then extracted with 80% ethanol (200 ml) for 4 times based on the Soxhlet extraction method. The filtrates were collected and transferred to a rotary evaporator. The crude extract was obtained after all of the solvent was dried up. Then, 20 ml ultrapure water was added and oscillated for 10 min to get the solution of crude extract. Half of the solution was taken out and dried by decompression rotary evaporation to obtain the total phase of the extract (tE-CJDC).10 ml petroleum ether was then added to the remaining crude extract solution, and transferred into a separatory funnel after fully shaking to completely dissolve the extract, standing for 20 min, collecting the upper petroleum ether phase solution and the lower water phase was extracted with 10 ml petroleum ether for two more times. The collected solution was dried by decompression rotary evaporation to get the petroleum ether phase extract which was named peE-CJDC. The remaining water phase solution was sequentially extracted with ethyl acetate and N-butyl alcohol following the same steps described above, and the products were named eaE-CJDC and nbaE-CJDC respectively. The remaining water phase solution after the above extraction was dried by decompression rotary evaporation to obtain the water phase extract (wE-CJDC).

2.3. Preparation of regenerated SF

Regenerated SF was synthesized according to previously reported methods. Briefly, cocoons were degummed in Na_2CO_3 (0.02 M) solution at 100 °C for three times to remove the sericin protein, 30 min each. After that, the dried silk was dissolved in 9.3 M LiBr solution with a water bath at 45 °C for half an hour. Then, the homogeneous solution was dialyzed (dialysis bag: MWCO = 1.4KD) against deionized water for 3 days. Finally, the regenerated SF was gained by filtering and lyophilizing the silk solution.

2.4. Fabrication and characterization of the composite nanofibrous matrices

Certain amount of SF, PEO and one of the extracts were dissolved in 4 ml 10% (V/V) glacial acetic acid solution (The final concentration of SF, PEO and the extracts was fixed at 20% (wt/v), 2% (wt/v) and 0.5% (wt/v), respectively). The mixtures were stirred over 10 h to obtain a stable spinning solution. And then these solutions were electrospun with a stable extruding rate of 1.2 ml h^{-1} under a voltage of +11 kV at a collection distance of 15 cm. The products of the electrospinning (tE-CJDC@SF, peE-CJDC@SF, eaE-CJDC@SF, nbaE-CJDC@SF and wE-CJDC@SF nanofibers matrices

were obtained, respectively) were treated with 75% (V/V) ethanol vapor to improve their crystallinity as described in the previous study [32]. And then the matrices were dried under vacuum for 24 h at room temperature.

The morphology of the nanofibrous matrices was characterized using scanning electron microscope (SEM, TM-1000, Japan), the samples were coated with gold film at 4 mA for 20 s before measurements. The composition of the matrices was also analyzed by Fourier transform infrared spectroscopy (FTIR, Avatar380, USA) in range from 4000 to 400 cm^{-1} wave numbers. The contact angle test was performed to characterize the hydrophilicity of the matrices using astatic contact angle measuring instrument (DSA30, Germany).

2.5. Cytocompatibility assessment *in vitro*

2.5.1. Cell culture

In vitro cytocompatibility of the nanofibrous matrices was assessed by MTT assay. L929 cells were cultured in RPMI 1640 medium (Invitrogen, USA) supplemented with 10% fetal bovine serum (Invitrogen, USA) and incubated in a humidified incubator at 37 °C, with 5% CO_2. The nanofibrous mats were collected on circular glass cover slips (14 mm in diameter) for cellular study. After treatment with 75% (v/v) ethanol vapor, nanofiber-deposited cover slips were placed into a 24-well culture plate and fixed with autoclaved stainless-steel rings (herein, nanofiber-free cover slips as controls). L929 cells were seeded on the nanofibrous mats at the same density of 1.0×10^4 cells/well. Initially, the volume of cells and medium was 400 μl for each well, and then 200 μl of fresh medium was added to each well every 3 days.

2.5.2. Cell viability assay

The cells were allowed to proliferate on the substrates for 1, 3, 5 and 7 days. At these specific time point, cell-seeded or unseeded nanofibrous mats and cover slips were rinsed with PBS for three times following medium being removed. Thereafter, each well was supplemented with 400 μl of serum-free Dulbecco's modified Eagle's medium (DMEM) (Invitrogen, USA) containing 0.5 mg ml^{-1} MTT (Sigma–Aldrich). After being cultured for 4 h, the medium was completely aspirated and the formazan formed was dissolved in 400 μl of dimethyl sulfoxide. Then 100 μl of the solution was withdrawn to measure the absorption at 492 nm with a microplate reader (Thermo, USA), and the background value of cell-unseeded nanofibrous mats or cover slips was taken out correspondingly.

2.5.3. Cell morphology observation

To further study the interaction between cells and the nanofibrous matrices, the morphology of the cells grown on the matrices was examined by fluorescence microscopy and SEM. L929 cells cultured on different materials was fixed with 4% paraformaldehyde at 4 °C for 30 min and rinsed by PBS. And then, L929 cells were treated with 0.1% (v/v) Triton X-100 for 5 min, rinsed by PBS, and treated with 2% (wt/v) bovine serum albumin (BSA) for 30 min Last, after rinsing by PBS for three times, cells were dyed by Alexa Fluor®568 Phalloidin for 30 min and DAPI for 15 min. Then the morphology of L929 cells was imaged using a fluorescence microscope (Olympus IX71). Meanwhile, the paraformaldehyde fixed cells were dehydrated using gradient ethanol and dried in a vacuum oven. Subsequently, the samples were sputter-coated with gold and observed using SEM (JSM-5600).

2.6. The hemolytic rate of the nanofibrous matrices

A certain amount of rabbit blood treated with 3.8% sodium citrate solution to obtain the anticoagulant rabbit blood. Blood was further centrifuged for 10 min at 4 °C, and the supernatant was collected as the poor platelet plasma (PPP). The nanofibrous matrices were immersed into physiological saline with a water bath at 37 °C for 30 min. After that, the samples were mixed with 0.2 ml rabbit blood suspension and incubated at 37 °C for 1 h, and then centrifuged at 1200 rpm for 5 min. The supernatant liquid was transferred to a 96 wells plate. The absorbance (A) of the samples at 540 nm was detected using a microplate reader (Thermo, USA). For the negative control, 10 ml saline was used, whereas the 10 ml distilled water was used for the positive control. The hemolytic rate was calculated by the following equation:

$$\text{Hemolytic rate} = \frac{\text{A(material)} - \text{A(negative control)}}{\text{A(positive control)} - \text{A(negative control)}} \times 100\%$$

2.7. Plasma recalcification profiles test

Plasma recalcification time of the matrices was detected according to the previously reported method [33]. The matrices, AGS (used as positive control) and gauze (used as a control for the SF nanofibrous matrices) were incubated with 500 μl PPP containing 0.025 mol L^{-1} $CaCl_2$ (no $CaCl_2$ for the negative control) in 24 well plates at 37 °C for 1 h. Then 100 μl of the media was transferred to 96 wells plate to detect absorbance (A) at 405 nm for 45 min, the data was recorded every 30 s.

2.8. Statistical analysis

All experiments were carried out at least three times and data were reported as mean ± standard deviation (SD). The error bar sin the figures are the SDs of the data. One-way ANOVA statistical analysis was performed with an Origin 8.0 (Origin Lab, USA). In all statistical analysis, a p-value of less than 0.05 was considered statistically significance.

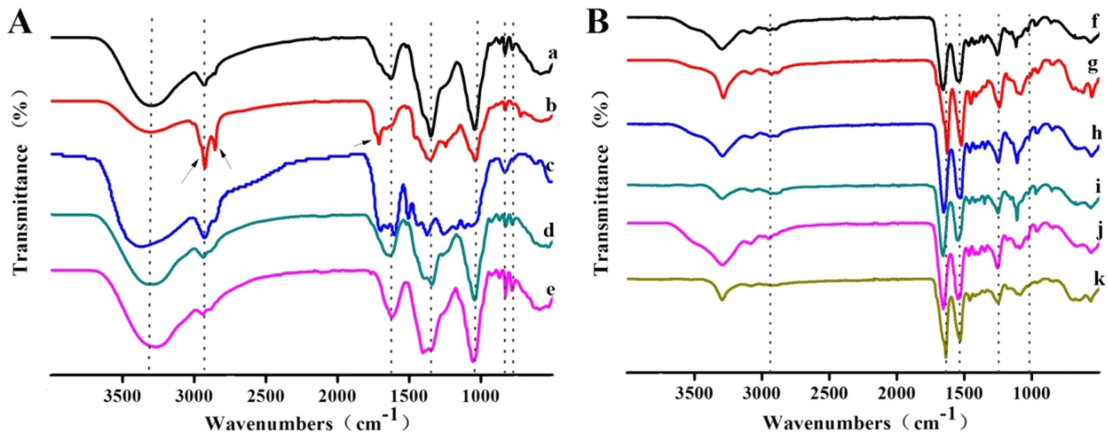

Figure 1. FTIR spectra of the CJDC extracts (A) and the extracts-loaded SF nanofibrous matrices (B) (a): tE-CJDC, (b): peE-CJDC, (c): eaE-CJDC, (d): nbaE-CJDC, (e): wE-CJDC, (f): tE-CJDC@SF, (g): peE-CJDC@SF, (h):eaE-CJDC@SF, (i): nbaE-CJDC@SF, (j): wE-CJDC@SF, (k):SF).

3. Results and discussion

3.1. Secondary structure of the CJDC extracts loaded SF nanofibrous matrices

The FTIR spectroscopy was used to study the composition of the matrices. As shown in figure 1(A), components of CJDC exhibited characteristic bands at 3000–3700 cm^{-1} (−OH), 2926 cm^{-1} (−CH_2- stretching vibration), 1650 cm^{-1} (C=O stretching vibration), 1345 cm^{-1} (C-H stretching vibration), 810–750 cm^{-1} (2,4-Di-substituted benzo stretching vibration) and 675 cm^{-1} (benzo) stretching vibration. Also, the difference between the components extracted with different methods was revealed. For instance, PE-CJDC displayed strong bands at 2928 cm^{-1} (−CH_2- stretching vibration), 2820 cm^{-1} and 1736 cm^{-1} (Aldehyde).

Figure 1(B) showed the spectra of the CJDC extracts-loaded SF nanofibers. The characteristic peaks at 1650–1660 cm^{-1} (amide I, C-O stretching vibration), 1535–1545 cm^{-1} (amide II, C-N stretching vibration and N-H bending vibration) and 1235–1240 cm^{-1} (amide III, C-N stretching vibration) belong to SF [32]. While the characteristic peaks at 3000–2900 cm^{-1} (−CH_2- stretching vibration) and 1150–1050 cm^{-1} (C-OH stretching vibration) were intensified in the spectra of the composite nanofibers, which may due to the impact of the CJDC extracts. Notably, the bands at1535–1545 cm^{-1} (amide II,) and 1250 cm^{-1} (amide III) shifted to a high wave number in the composite nanofibers compared with that of SF. Obviously, the characteristic peaks of both CJDC extracts and SF were presented in the composite nanofibers, which demonstrated that the CJDC extracts were successfully loaded into the SF nanofibers.

3.2. Morphology of the CJDC extracts loaded SF nanofibrous matrices

SEM was used to investigate the morphology of the composite nanofibrous matrices. As shown in figure 2, all the samples exhibited smooth and uniform fibers. The average diameter of the neat SF nanofibers was measured to be 299 ± 86 nm. While the diameters of the fibers were increased significantly with the incorporation of CJDC extracts (from 329 ± 88 nm to 529 ± 171 nm), probably due to the poor insolubility of CJDC extracts in aqueous solution which increase the viscosity of the SF/PEO solution at some extent. The narrow diameter of the composite nanofibers may be beneficial to the release of extracts [34].

3.3. The surface wettability of the CJDC extracts loaded SF nanofibrous matrices

The surface wettability affects the biocompatibility and protein adsorption capacity of the materials [35]. The hydrophilic surface can largely resist the adsorption of nonspecific protein, which in turn enhance cell infiltration and influence response between cell and foreign body [30, 36, 37]. Thus, it is important to assess the hydrophilic-hydrophobic property of the biomaterial. Here, the water contact angles were measured to characterize the surface wettability of the matrices. As summarized in figure 3, the water contact angles of all the samples were less than 90° (35°,34°, 38°, 24°, 23° and 30° corresponding to SF, tE-CJDC@SF, peE-CJDC@SF, eaE-CJDC@SF, nbaE-CJDC@SF and wE-CJDC@SF, respectively). When compared with the neat SF, the hydrophobicity of peE-CJDC@SF increased, whereas the hydrophilicity of other groups decreased. This result showed that the CJDC extracts loaded SF nanofibrous matrices have good surface hydrophilicity, which should be beneficial to the tissue regeneration.

3.4. Cytocompatibility of the CJDC extracts loaded SF nanofibrous matrices

The cell proliferation on the matrices was determined by MTT assay on day 1, 3, 5 and 7. As shown in figure 4, the skin fibroblasts grew and proliferated well on the CJDC extracts loaded SF nanofibrous matrices, much

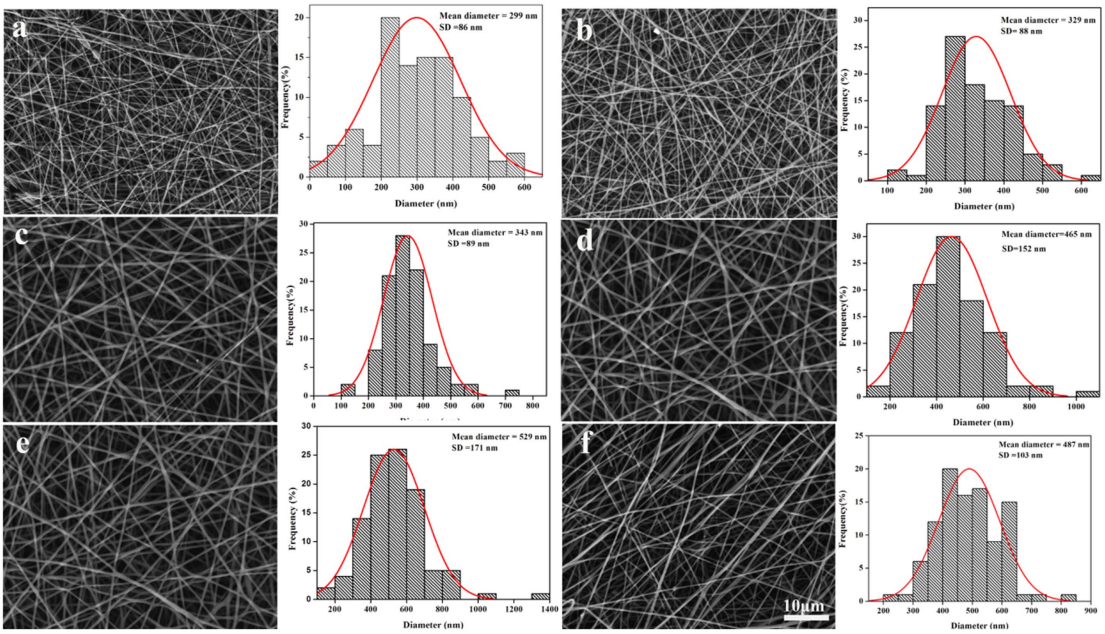

Figure 2. SEM images and diameter distributions of the CJDC extracts-loaded nanofibrous matrices (a): SF, (b): tE-CJDC@SF, (c): peE-CJDC@SF, (d): eaE-CJDC@SF, (e): nbaE-CJDC@SF, (f): wE-CJDC@SF).

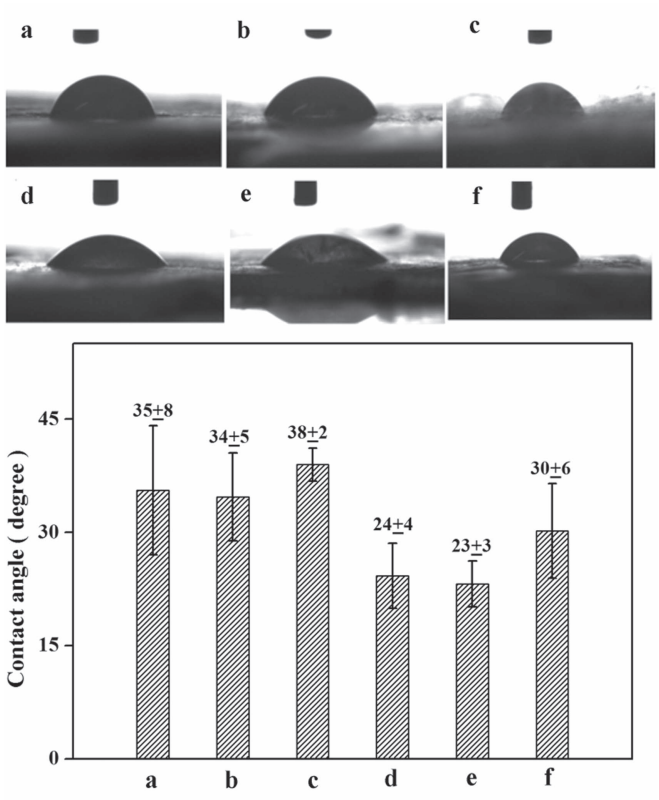

Figure 3. The surface wettability of the CJDC extracts loaded SF nanofibrous matrices (a): SF; (b): tE-CJDC@SF; (c): peE-CJDC@SF; (d): eaE-CJDC@SF; (e): nbaE-CJDC@SF; (f): wE-CJDC@SF).

better than that on the glass ($P < 0.05$), which should mainly attributed to SF as well as the mesh structure [38, 39]. Moreover, the incorporation of CJDC extracts seemed beneficial to the proliferation of the skin cells considering that the cell viability on the CJDC extracts loaded SF nanofibrous matrices (excepts the group of tE-CJDC@SF) at day 7 was better than that on the neat SF matrices. The flavonoids have been reported to be the main pharmacological constituents in CJDC [26–28]. Flavonoids have good

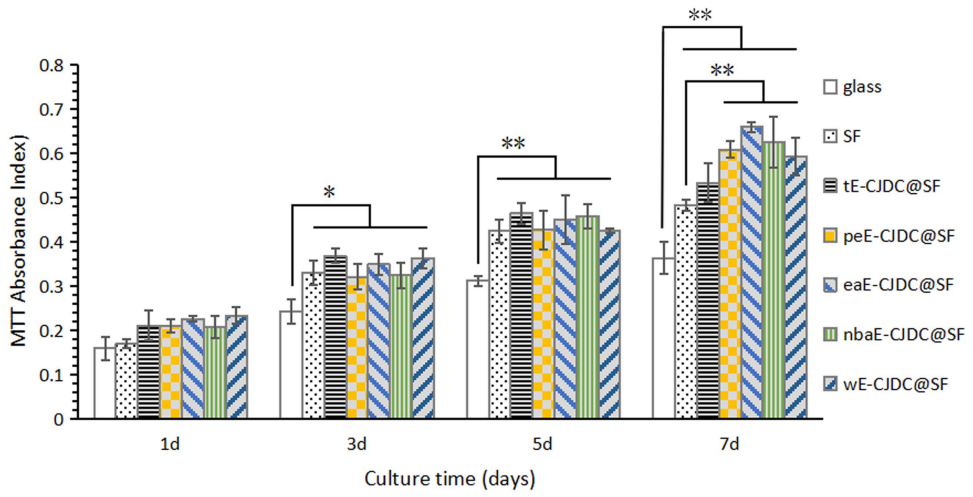

Figure 4. The viability of L929 cells grown on different substrates ($^{*}p < 0.05$, $^{**}p < 0.01$).

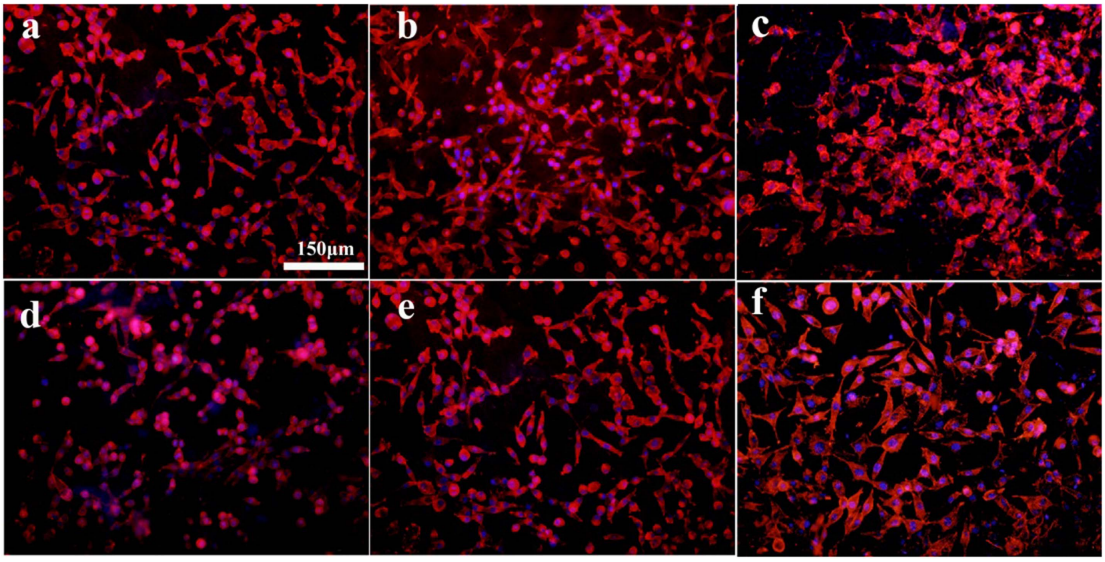

Figure 5. The fluorescence microscopy images of L929 cells grown on different materials (a): SF; (b): tE-CJDC@SF; (c): peE-CJDC@SF; (d): eaE-CJDC@SF; (e): nbaE-CJDC@SF; (f): wE-CJDC@SF).

antioxidant effect, which may explain the significant increase of the viability of the cells grown on the CJDC extracts loaded SF nanofibrous matrices compared with the neat SF matrices.

Subsequently, cell phenotype on the matrices was also investigated by fluorescence microscopy. As shown in figure 5, after3 days' culture, the skin cells grown on the composite matrices typically took a fusiform morphology and started bridging each other to form a large cell area. The phenotype of the cells grown on the matrices was further revealed by SEM (shown in figure 6). The cells can be clearly seen robustly attached and expanding filopodia on the nanofibrous matrices with porous mesh structure, suggesting a nice material-cells and cell-cell signal conduction [39]. These data indicated that the CJDC extracts loaded SF nanofibrous matrices have a good cytocompatibility.

3.5. Hemolysis ratio test of the CJDC extracts loaded SF nanofibrous matrices

The hemolysis rates assay was conducted by the standard method according to the American society for testing and materials. The standard classified the hemolysis of material as non-hemolytic (0%–2%), slightly hemolytic (2%–5%) and hemolytic (>5%) [33]. As shown in figure 7, the hemolysis rates were 1.9%, 1.2%, 0.9%, 1.3%, 2.1% and 1.1% corresponding to SF, tE-CJDC@SF, peE-CJDC@SF, eaE-CJDC@SF, nbaE-CJDC@SF and wE-CJDC@SF, respectively. Among the tested groups, the peE-CJDC@SF had the best performance, while the nbaE-CJDC@SF showed a slightly hemolytic. In general, our data indicated the CJDC extracts loaded SF composite nanofibrous matrices have a good hemocompatibility.

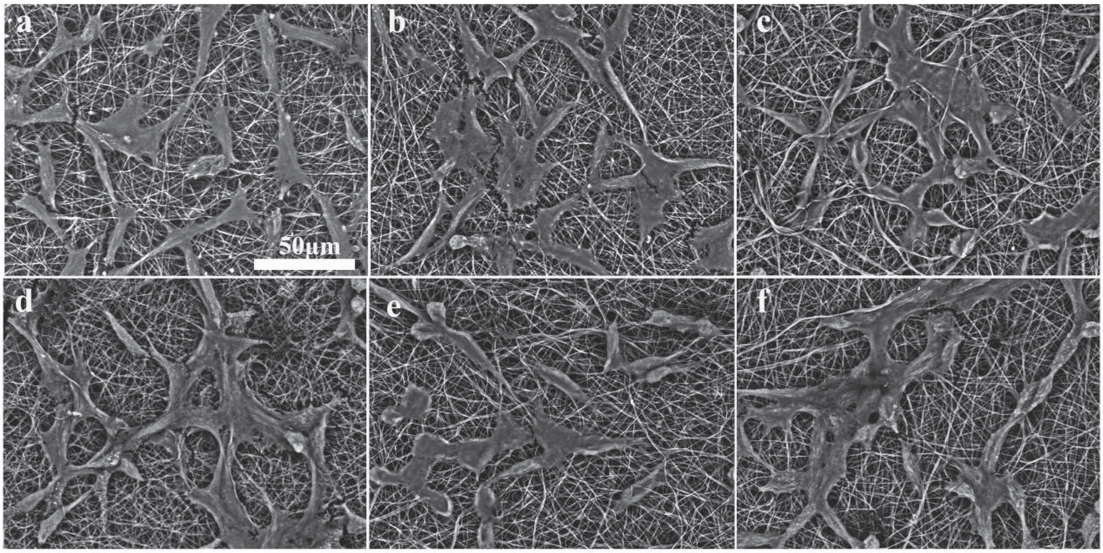

Figure 6. The SEM images (1000×) of L929 cells grown on different materials (a): SF; (b): tE-CJDC@SF; (c): peE-CJDC@SF; (d): eaE-CJDC@SF; (e): nbaE-CJDC@SF; (f): wE-CJDC@SF).

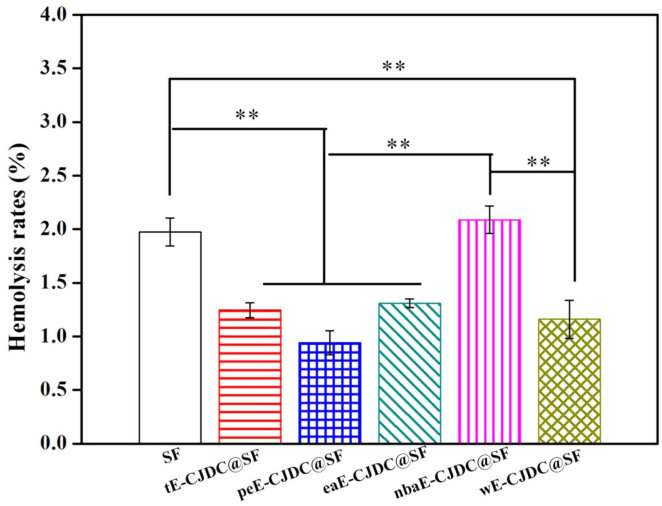

Figure 7. The hemolysis rates of different materials ($^{*}p < 0.05$, $^{**}p < 0.01$).

3.6. Plasma recalcification profile

The activation of the intrinsic pathway of coagulation was determined by the response assay of adding PPP to a material. The absorbance increased with the increase of plasma turbidity, correlating with the formation of clots. The stringent time in this measure was represented by the time when half the maximum absorbance was achieved. The time value smaller, the coagulation capability of the material better. For the negative comparison group, the PPP without $CaCl_2$ was used, whereas the other groups included $CaCl_2$ [40–43]. As shown in figure 8, the blood clotting time corresponding to AHG, AGS, tE-CJDC@SF, peE-CJDC/SF, eaE-CJDC@SF, nbaE-CJDC@SF, wE-CJDC@SF and SF were 16 min, 15.75 min, 9.5 min, 19.25 min, 22 min, 21.25 min and 26.75 min respectively. These data indicated that the incorporation of CJDC extracts can significantly improve blood clotting activity of the SF nanofibrous matrices. What's exciting was the performance of the peE-CJDC@SF nanofibrous matrices possessing a time value of only 9.5 min, which is much better than the performance of the positive controls (AHG and AGS).

Interestingly, the half maximum absorbance time for general gauze was over 45 min, much longer than that of the neat SF nanofibrous matrices, suggesting the hemostatic activity of SF is much better than that of the general gauze. Thus, the SF nanofiber-based materials should be superior to gauze when using for hemostasis. CJDC has exact anti-inflammatory, analgesic, anti-bacterial and hemostatic effects and is widely used in Chinese traditional medicine [26–28]. The main pharmacological constituents in CJDC had been reported to be the flavonoid. Of them, the

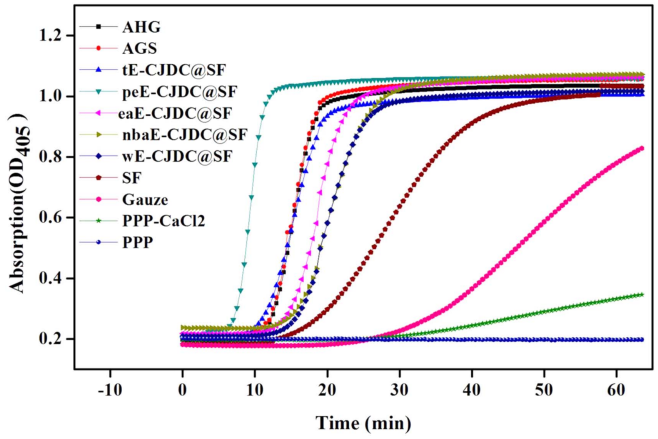

Figure 8. The restringent time of different material.

linarin, pectolinarin and pectolinarigenin have been proven to be the main ingredients responsible for the hemostatic activity in CJDC [44, 45]. In our extraction, the content of linarin, pectolinarin or pectolinarigenin should be higher in the peE-CJDC than in other phase, which may explain why peE-CJDC/SF had the best hemostatic performance among the groups. According to our data, the hemostatic activity of peE-CJDC/SF nanofibrous matrices was even much better than that of AHG and AGS (both are widely used hemostatic products in clinic). As demonstrated earlier, the peE-CJDC/SF nanofibrous matrices also have excellent cytocompatibility and hemocompatibility. Taking all into account, the peE-CJDC/SF nanofibrous matrices can be a good candidate for wound dressing with excellent hemostatic activity.

4. Conclusions

In this study, a kind of SF nanofibrous matrices loading CJDC ingredients was fabricated by green electrospinning and characterized in detail. Theasspun composite matrices had a porous mesh structure and showed good cytocompatibility as well as hemocompatibility. Furthermore, the incorporaton of CJDC ingredients was demonstrated to significantly improve the cytocompatibility and hemostatic performance of the SF nanofibrous matrices. Satisfactorily, among the as-spun products, the peE-CJDC@SF nanofibrous matrices showed the best antihemorrhagic activity (with a stringent time of 9.5 min), which was even superior to some clinic hemostatic product such as AHG and AGS. Our data suggested the CJDC extracts loaded SF nanofibrous matrices, especially the peE-CJDC@SF nanofibrous matrices, have promising potential used as hemostatic material and wound dressing.

Acknowledgments

This research was supported by Open Foundation of Key Laboratory of Science & Technology of Eco-Textile (Eco-KF-201612), Shanghai Science and Technology Committee Project (15430502700), Shanghai Education Committee Fund (16SG38), Zhejiang Provincial Science and Technology Department Public Technology Application Research Program (Grant No.2015C33285) and Zhejiang Provincial Natural Science Foundation of China (Grant No. LY14H300002).

ORCID iDs

Linlin Ma https://orcid.org/0000-0002-4908-3607

References

[1] Li C *et al* 2013 Silver nanoparticle/chitosan oligosaccharide/poly(vinyl alcohol) nanofibers as wound dressings: a preclinical study *Int. J. Nanomed.* **2013** 4131–45
[2] Anumolu S S *et al* 2011 Doxycycline hydrogels with reversible disulfide crosslinks for dermal wound healing of mustard injuries *Biomater.* **32** 1204–17
[3] Kumar P T, Lakshmanan V K, Biswas R, Nair S V and Jayakumar R 2012 Synthesis and biological evaluation of chitin hydrogel/nano ZnO composite bandage as antibacterial wound dressing *J. Biomed. Nanotech.* **8** 891
[4] Recinos G, Inaba K, Dubose J, Demetriades D and Rhee P 2008 Local and systemic hemostatics in trauma: a review *Ulusal Travma ve acil cerrahi Dergisi = Turkish Journal of Trauma & Emergency Surgery: TJTES* **14** 175
[5] Whang H S, Kirsch W, Zhu Y H, Yang C Z and Hudson S M 2005 Hemostatic agents derived from chitin and chitosan *Polym. Rev.* **45** 309–23
[6] Ishihara M *et al* 2002 Photocrosslinkable chitosan as a dressing for wound occlusion and accelerator in healing process *Biomater.* **23** 833
[7] Lima P H *et al* 2013 Blood protein adsorption on sulfonated chitosan and κ-carrageenan films *Colloids & Surfaces B Biointerfaces* **111** 719–25
[8] Chemi A 2009 A new hemostatic agent: initial life-saving experience with Celox (chitosan) in cardiothoracic surgery *Annals. Thorac. Surg.* **87** 13–4

[9] Monteiro N et al 2015 Antibacterial activity of chitosan nanofiber meshes with liposomes immobilized releasing gentamicin *Acta Biomater.* **18** 196
[10] Aboushwareb T et al 2009 A keratin biomaterial gel hemostat derived from human hair: evaluation in a rabbit model of lethal liver injury *J. Biomed. Mater. Res. Part B Applied Biomaterials* **90** 45
[11] Ellisbehnke R G et al 2006 Nano hemostat solution: immediate hemostasis at the nanoscale *Nanomed. Nanotech. Bio. Med.* **2** 207
[12] Dhulkotia J S, Alazzam M and Galimberti A 2009 Tisseel for management of traumatic postpartum haemorrhage *Arch. Gynecol. Obstet.* **279** 437–9
[13] Vaiman M, Sarfaty S and Eviatar E 2009 The use of fibrin sealant as a glue for septoplasty and conchotomy *Rhinology* **47** 297–300
[14] Mogford J E, Tawil B, Jia S and Mustoe T A 2009 Fibrin sealant combined with fibroblasts and platelet-derived growth factor enhance wound healing in excisional wounds *Wound Repair and Regeneration* **17** 405–10
[15] Descottes B and D'Arc M B 2009 Fibrin sealant in inguinal hernioplasty: an observational multicentre study in 1201 patients *Hernia* **13** 505–10
[16] Kavanagh M, Ohr M, Czyz C N, Cahill K, Perry J, Holck D and Foster J 2009 Comparison of fibrin sealant versus suture for wound closure in Muller muscle-conjunctiva resection ptosis repair *Ophthalmic Plastic & Reconstructive Surgery* **25** 99–102
[17] Min B M, Lee G, Kim S H, Nam Y S, Lee T S and Park W H 2004 Electrospinning of silk fibroin nanofibers and its effect on the adhesion and spreading of normal human keratinocytes and fibroblasts *in vitro Biomater.* **25** 1289
[18] Guziewicz N, Best A, Perez-Ramirez B and Kaplan D L 2011 Lyophilized silk fibroin hydrogels for the sustained local delivery of therapeutic monoclonal antibodies *Biomater.* **32** 2642
[19] Melke J, Midha S, Ghosh S, Ito K and Hofmann S 2016 Silk fibroin as biomaterial for bone tissue engineering *Acta Biomaterialia* **31** 1–16
[20] Fan L et al 2014 Green electrospun pantothenic acid/silk fibroin composite nanofibers: fabrication, characterization and biological activity *Colloids & Surfaces B Biointerfaces* **117** 14–20
[21] Calamak S, Erdoğdu C, Ozalp M and Ulubayram K 2014 Silk fibroin based antibacterial bionanotextiles as wound dressing materials *Mater. Sci. Eng.* C **43** 11
[22] Calamak S, Aksoy E A, Ertas N, Erdogdu C, Sagıroglu M and Ulubayram K 2015 Ag/silk fibroin nanofibers: effect of fibroin morphology on Ag + release and antibacterial activity *Eur. Polym. J.* **67** 99–112
[23] Yang X et al 2017 Green electrospun Manuka honey/silk fibroin fibrous matrices as potential wound dressing *Mater. Des.* **119** 76–84
[24] Cai Z X et al 2010 Fabrication of chitosan/silk fibroin composite nanofibers for wound-dressing applications *Int. J. Mol. Sci.* **11** 3529–39
[25] Song D W, Kim S H, Kim H H, Lee K H, Ki C S and Park Y H 2016 Multi-biofunction of antimicrobial peptide-immobilized silk fibroin nanofiber membrane: implications for wound healing *Acta Biomaterialia* **39** 146–55
[26] Lin C, Arisawa M, Shimizu M and Morita N 2008 The constituents of Cirsium Japonicum DC var. takaoense Kitamura isolation of two new flavonoids, cirsitakaoside (IV) and cirsitakaogenin (VI) *Pharmaceutical Bulletin* **26** 2036–9
[27] Park J C, Lee J H and Choi J S 1995 A flavone diglycoside from Cirsium Japonicum var. ussuriense *Phytochemistry* **39** 261–2
[28] Kim S J and Kim G H 2003 Identification for flavones in different parts of Cirsium japonicum *Preventive Nutrition & Food Science* **8** 330–5
[29] Miyaichi Y, Matsuura M and Tomimori T 1995 Phenolic Compound from the roots of Cirsium Japonicum DC *Nat. Med.* **49** 92–4
[30] Beek M V, Jones L and Sheardown H 2008 Hyaluronic acid containing hydrogels for the reduction of protein adsorption *Biomater.* **29** 780–9
[31] Takaishi Y, Okuyama T, Nakano K, Murakami K and Tomimatsu T 1991 Absolute configuration of a triolacetylene from Cirsium japonicum *Phytochemistry* **30** 2321–4
[32] Wang H 2012 Regenerated silk fibroin nanofibrous matrices treated with 75% ethanol vapor for tissue-engineering applications *J. Biomater. Sci., Polym. Ed.* **23** 497
[33] Motlagh D, Yang J, Lui K Y, Webb A R and Ameer G A 2006 Hemocompatibility evaluation of poly(glycerol-sebacate) *in vitro* for vascular tissue engineering *Biomater.* **27** 4315–24
[34] Zhu T, Yang C, Chen S, Li W, Lou J and Wang J 2015 A facile approach to prepare shell/core nanofibers for drug controlled release *Mater. Lett.* **150** 52–4
[35] Dobrovolskaia M A and Mcneil S E 2007 Immunological properties of engineered nanomaterials *Nat. Nanotechnol.* **2** 469–78
[36] Peppas N A, Hilt J Z, Khademhosseini A and Langer R 2006 Hydrogels in biology and medicine: from molecular principles to bionanotechnology *Adv. Mater.* **18** 1345–60
[37] Emanuele O et al 2001 Self-assembled monolayers that resist the adsorption of proteins and the adhesion of bacterial and mammalian cells *Langmuir* **17** 6336–43
[38] Sheng X, Fan L, He C, Zhang K, Mo X and Wang H 2013 Vitamin E-loaded silk fibroin nanofibrous mats fabricated by green process for skin care application *Int. J. Biol. Macromol.* **56** 49
[39] Fan L et al 2012 Vitamin C-reinforcing silk fibroin nanofibrous matrices for skin care application *Rsc. Advances* **2** 4110–9
[40] Sperling C, Fischer M, Maitz M F and Werner C 2009 Blood coagulation on biomaterials requires the combination of distinct activation processes ⋆ *Biomater.* **30** 4447
[41] Gupta S and Reviakine I 2012 Platelet activation profiles on TiO 2: effect of Ca 2+ binding to the surface *Biointerphases* **7** 28
[42] Andrade F K, Silva J P, Carvalho M, Castanheira E M, Soares R and Gama M 2013 Studies on the hemocompatibility of bacterial cellulose *J. Bioact. Compat. Polym.* **28** 97–112
[43] Ryu K E et al 2003 Plasma protein adsorption to anion substituted poly(vinyl alcohol) membranes *Macromol. Res.* **11** 451–7
[44] Zhi F, Kong L-Y and Peng S-S 2003 Studies on the chemical constituents of Cirsium Japonicum DC *Acta Pharmaceutica Sinica* **38** 442–7
[45] Zhong L-Y, Zheng H, Gong Q-F and Ding X 2011 Initial study on pharmacodynamic substance with haemostasis in Charred Japanese thistle herb *China Journal of Traditional Chinese Medicine and Pharmacy* **26** 147–9